Astronomy
&
Astrophysics

Pulsations powered by hydrogen shell burning in white dwarfs

M. E. Camisassa[1,2], A. H. Córsico[1,2], L. G. Althaus[1,2], and H. Shibahashi[3]

[1] Grupo de Evolución Estelar y Pulsaciones. Facultad de Ciencias Astronómicas y Geofísicas, Universidad Nacional de La Plata, Paseo del Bosque s/n, 1900 La Plata, Argentina
e-mail: camisassa@fcaglp.unlp.edu.ar
[2] Instituto de Astrofísica de La Plata, Centro Científico Tecnológico La Plata, Consejo Nacional de Investigaciones Científicas y Técnicas, Paseo del Bosque s/n, 1900 La Plata, Argentina
[3] Department of Astronomy, The University of Tokyo, Bunkyo-ku, Tokyo 113-0033, Japan

ABSTRACT

Context. In the absence of a third dredge-up episode during the asymptotic giant-branch phase, white dwarf models evolved from low-metallicity progenitors have a thick hydrogen envelope, which makes hydrogen shell burning be the most important energy source.

Aims. We investigate the pulsational stability of white dwarf models with thick envelopes to see whether nonradial g-mode pulsations are triggered by hydrogen burning, with the aim of placing constraints on hydrogen shell burning in cool white dwarfs and on a third dredge-up during the asymptotic giant-branch evolution of their progenitor stars.

Methods. We construct white-dwarf sequences from low-metallicity progenitors by means of full evolutionary calculations that take into account the entire history of progenitor stars, including the thermally pulsing and the post-asymptotic giant-branch phases, and analyze their pulsation stability by solving the linear, nonadiabatic, nonradial pulsation equations for the models in the range of effective temperatures $T_{\rm eff} \sim 15\,000-8000$ K.

Results. We demonstrate that, for white dwarf models with masses $M_\star \lesssim 0.71\,M_\odot$ and effective temperatures $8500 \lesssim T_{\rm eff} \lesssim 11\,600$ K that evolved from low-metallicity progenitors ($Z = 0.0001, 0.0005,$ and 0.001), the dipole ($\ell = 1$) and quadrupole ($\ell = 2$) g_1-modes are excited mostly as a result of the hydrogen-burning shell through the ε-mechanism, in addition to other g-modes driven by either the $\kappa - \gamma$ or the convective driving mechanism. However, the ε mechanism is insufficient to drive these modes in white dwarfs evolved from solar-metallicity progenitors.

Conclusions. We suggest that efforts should be made to observe the dipole g_1-mode in white dwarfs associated with low-metallicity environments, such as globular clusters and/or the galactic halo, to place constraints on hydrogen shell burning in cool white dwarfs and the third dredge-up episode during the preceding asymptotic giant-branch phase.

Key words. stars: evolution – stars: interiors – stars: oscillations – white dwarfs

1. Introduction

White dwarf stars are the most common end product of stellar evolution, with 97% of all stars becoming white dwarfs. As a result, observations of white dwarfs provide us with rich information about the stellar evolution of their progenitors and the star-formation history in our galaxy. Furthermore, some white dwarfs are pulsating stars, hence asteroseismology of these stars makes further information available about the internal structure and the evolutionary status of white dwarfs. Several types of pulsating white dwarfs have been observed: GW Vir (pulsating PG1159) stars, hot DA variable (HDAV) stars, V777 Her (DBV) stars, hot DQ variable (HDQV) stars, ZZ Ceti (DAV) stars, and extremely low mass variable (ELMV) stars (Winget & Kepler 2008; Fontaine & Brassard 2008; Althaus et al. 2010; Fontaine et al. 2013). They exhibit luminosity variations with periods ranging from ∼100 s to ∼6000 s, which are attributed to nonradial g-modes excited by either the $\kappa - \gamma$ mechanism that works in the ionization zones of the abundant chemical elements or convection in cool white dwarfs (Brickhill 1983; Goldreich & Wu 1999).

Besides those mechanisms, the ε mechanism has been predicted to lead to destabilization of some short-period g-modes in white-dwarf and pre-white-dwarf stars. This mechanism is induced by thermonuclear reactions, which are highly dependent on temperature. During a compression phase, the temperature and thus the nuclear energy production rates are higher than at equilibrium, hence, in the layers where nuclear reactions take place, more thermal energy is produced. The opposite occurs during the following expansion phase, and as a consequence, the contribution of the perturbation of nuclear energy generation to the work integral is always a destabilization effect (Unno et al. 1989). The first study of the ε mechanism in pre-white-dwarf stars was the seminal work by Kawaler et al. (1986), who found that some g-modes with periods in the range 70−200 s are indeed excited through this mechanism by helium shell burning in hydrogen-deficient pre-white-dwarf stars. Later on, Córsico et al. (2009) conducted a more thorough stability analysis, and showed the existence of an instability strip for GW Vir stars in the H–R diagram, for which the ε mechanism by helium shell burning is responsible. As for hydrogen burning, Maeda & Shibahashi (2014) recently predicted that some low-order g-modes are excited by the ε mechanism due to vigorous hydrogen shell burning in very hot and luminous pre-white dwarfs with hydrogen-rich envelopes. Also, Córsico & Althaus (2014) have shown that some low-order g-modes could be driven in ELMVs

by the ε mechanism due to hydrogen shell burning, although most of the observed pulsation modes, which are characterized by high- and intermediate-radial orders, are likely to be excited by the $\kappa - \gamma$ mechanism.

Recent detailed studies by Miller Bertolami et al. (2013) and Althaus et al. (2015) have shown that white dwarf stars evolved from low-metallicity progenitors ($0.00003 \lesssim Z \lesssim 0.001$), in the absence of carbon enrichment due to third dredge-up episodes during the asymptotic giant-branch (AGB) phase, have a thick enough hydrogen envelope, which makes stable hydrogen shell burning by pp-chain the most important energy source even at low luminosities ($\log L/L_\odot \lesssim -3$). Nuclear burning becomes weaker with an increase of metallicity. The importance of hydrogen shell burning is also strongly dependent on the mass of the white dwarf, and no significant burning is expected to occur in white dwarfs with masses greater than $\sim 0.6\,M_\odot$. This extra source of energy delays the white dwarf cooling. Even at low luminosities, $\log L/L_\odot \sim -4$, residual hydrogen burning leads to an increase in the cooling times of the low- and intermediate-mass white dwarfs ($M \lesssim 0.6\,M_\odot$) by ~ 20–40%. These results are not affected by the mass loss rate in the preceding stages. On the other hand, the occurrence of overshooting during the AGB phase strongly favors third dredge-up episodes. This leads to the formation of white dwarfs with thinner hydrogen envelopes, with the consequence that no appreciable residual hydrogen burning during the white dwarf regime is expected. The delay of the cooling times of white dwarfs evolved from low-metallicity progenitors impacts on our understanding of stellar populations. In particular, Torres et al. (2015) employed the observed white dwarf luminosity function of the low-metallicity globular cluster NGC 6397 to constrain the hydrogen nuclear burning in white dwarfs from low-metallicity progenitors. They conclude that the low-mass white dwarf population in NGC 6397 should be characterized by important residual burning and hence, the progenitors of these stars should not have experienced third dredge-up in the AGB phase. Although Cojocaru et al. (2015) tried the same with the isolated white dwarfs in the galactic halo, they could not reach a definitive conclusion, because the number of detected white dwarfs in the galactic halo remains too small.

According to Miller Bertolami et al. (2013) and Althaus et al. (2015), the contribution of nuclear energy generation to the luminosity of the white dwarfs evolved from low-metallicity progenitors is the largest, being about 80% of the luminosity of the star, when $\log T_{\rm eff} \sim 4$. It is in this effective temperature range that many DAVs are found to pulsate in g-modes driven by either the $\kappa - \gamma$ mechanism or the convective driving mechanism. Motivated by these results, in this paper we assess the possibility that DA white dwarfs belonging to low-metallicity stellar populations (like globular clusters and the galactic halo) can develop short-period variabilities, analogous to the short-period g-modes exhibited by ZZ Ceti stars. As described above, the low-mass and low-metallicity progenitors of this kind of DA white dwarfs should avoid the third dredge-up episodes in the AGB phase, such that residual hydrogen burning continues at a significant level, and overstability of g-modes is induced by the ε mechanism. Along this study, we aim to use white dwarf pulsations to verify the presence of hydrogen shell burning in some white dwarfs, and eventually, to constrain the efficiency of third dredge-up episodes in the AGB phase.

The paper is organized as follows: in Sect. 2 we briefly describe our stellar evolution and stellar pulsation tools and the main ingredients of the evolutionary sequences. In Sect. 3 we present our pulsation results in detail. Finally, in Sect. 4 we summarize our main findings.

2. Evolutionary models and numerical tools

We constructed equilibrium models of low-mass white dwarfs evolved from low-metallicity progenitors, using the LPCODE stellar evolutionary code (Althaus et al. 2003, 2005, 2012, 2015; Camisassa et al. 2016), which were initially evolved from the zero age main sequence (ZAMS), all the way to the white-dwarf stage. Additionally, we computed an evolutionary sequence of solar metallicity ($Z = 0.018$) in order to see if the ε mechanism could also excite oscillations in white dwarfs coming from solar-metallicity progenitors. The physical inputs of our models were described in detail by Althaus et al. (2015). Below, we list the main ingredients which are relevant for this work:

- Extra mixing due to diffusive convective overshooting has been considered during the core hydrogen and helium burning phases. Following Althaus et al. (2015), extra mixing was not considered during the thermally-pulsing AGB. The overshooting parameter was set to $f = 0.015$ at each convective boundary.
- Mass loss during the red giant-branch phase was taken from Schröder & Cuntz (2005). For the AGB phase, we use again that of Schröder & Cuntz (2005) for pulsation periods shorter than 50 days. For longer periods, mass loss is taken as the maximum of the rates of Schröder & Cuntz (2005) and Groenewegen et al. (2009) for oxygen rich stars, or the maximum of the rates of Schröder & Cuntz (2005) and Groenewegen et al. (1998) for carbon-rich stars. In all of our calculations, mass loss was suppressed after the post-AGB remnants reach $\log T_{\rm eff} = 4$.
- Radiative and conductive opacities are taken from OPAL (Iglesias & Rogers 1996) and from Cassisi et al. (2007), respectively. For the low-temperature regime we used molecular opacities with varying carbon to oxygen ratios (C/O) (Ferguson et al. 2005; Weiss & Ferguson 2009). These opacities are necessary for a realistic treatment of progenitor evolution during the thermally-pulsing AGB phase.
- For the white-dwarf stage we employed an updated version of the equation of state of Magni & Mazzitelli (1979) for the low-density regime, whereas for the high-density regime we considered the equation of state of Segretain et al. (1994).
- Changes in the chemical abundances have been computed consistently with the predictions of nuclear burning and convective mixing all the way from the ZAMS to the white dwarf phase. In addition, abundance changes resulting from atomic element diffusion were considered during the white dwarf regime.
- For the white-dwarf stage and for effective temperatures lower than $10\,000\,$K, outer boundary conditions for the evolving models are derived from non-gray model atmospheres (Rohrmann et al. 2012).

Table 1 lists the initial masses of the sequences, the resulting white dwarf masses, the hydrogen mass fraction, $\log\,(M_{\rm H}/M_\odot)$, and the surface C/O ratio at the beginning of the white dwarf phase. Our prediction for the initial-to-final mass relation is similar to that calculated by Romero et al. (2015). The C/O ratio indicates that, with the exception of the $M_\star = 0.738\,M_\odot$ sequence with $Z = 0.0001$, none of these model stars experienced carbon enrichment of the envelope during the AGB phase. The total amount of hydrogen at the beginning of the white dwarf

Table 1. Basic model properties for sequences with $Z = 0.0001, 0.0005,$ 0.0010 and 0.0180.

Z	$M_{\mathrm{ZAMS}}(M_\odot)$	$M_{\mathrm{WD}}(M_\odot)$	$\log(M_{\mathrm{H}}/M_\odot)$	C/O
0.0001	0.85	0.535	−3.304	0.301
0.0005	0.80	0.509	−3.231	0.241
0.0010	0.85	0.538	−3.434	0.307
0.0180	1.00	0.521	−3.543	0.005
0.0001	1.50	0.666	−3.851	0.264
0.0001	2.00	0.738	−4.347	11.477

Notes. M_{ZAMS}: initial mass, M_{WD}: white dwarf mass, $\log(M_{\mathrm{H}}/M_\odot)$: logarithm of the mass of the hydrogen envelope at the maximum effective temperature at the beginning of the cooling branch, C/O: surface carbon to oxygen mass ratio at the beginning of the cooling branch.

stage (M_{H}) is a key quantity for assessing the importance of nuclear burning, since the more massive the hydrogen envelope is, the more intense the burning is. In this work, we have not considered that some white dwarfs could have thin hydrogen envelopes (Castanheira & Kepler 2008, 2009; Romero et al. 2012, 2013)

The pulsation computations were performed with the linear, nonradial, nonadiabatic version of the LP–PUL pulsation code described by Córsico et al. (2006; see also Córsico et al. 2009). Although we have considered both dipole ($\ell = 1$) and quadrupole ($\ell = 2$) g-modes, the results are qualitatively similar and therefore we will focus on results for $\ell = 1$. The pulsation code solves the sixth-order complex system of linearized equations and boundary conditions as given by Unno et al. (1989). The code considers the mode excitation by both the $\kappa - \gamma$ mechanism and the ε mechanism. Our computations ignore the perturbation of the convective flux, that is, we are adopting the frozen-in convection approximation. While this approximation is known to give unrealistic locations of the g-mode red edge of the ZZ Ceti instability strip, it leads to satisfactory predictions for the location of the blue edge (Van Grootel et al. 2012; Saio 2013). The same is true for the blue edge of the instability domain of the ELMV stars (Córsico & Althaus 2016). We have also performed additional calculations disregarding the effects of nuclear energy release on the nonadiabatic pulsations, for which we fix $\varepsilon = \varepsilon_\rho = \varepsilon_T = 0$, where ε is the nuclear energy production rate, and ε_ρ and ε_T are their logarithmic derivatives, defined as $\varepsilon_\rho = (\partial \ln \varepsilon / \partial \ln \rho)_T$ and $\varepsilon_T = (\partial \ln \varepsilon / \partial \ln T)_\rho$, respectively. In this way, we prevent the ε mechanism from operating, although nuclear burning was still taken into account in the evolutionary computations.

While the temperature dependence of energy generation all through the pp-chain in equilibrium is governed by the slowest reaction between two protons and $\varepsilon_T \simeq 4$, we adopted the effective temperature dependence of nuclear reaction through the perturbation, which is mainly governed by ^{3}He-^{3}He reaction and $\varepsilon_T \simeq 11$ (Unno et al. 1989).

3. Results

Our stability analysis indicates the existence of many unstable g-modes in all the white dwarf model sequences, most of the modes being destabilized by the $\kappa - \gamma$ mechanism acting at the surface hydrogen ionization zone. From observations, we know that as the ZZ Ceti stars cool inside the instability strip, modes with progressively higher radial orders are excited. This can be understood theoretically on the basis of the thermal

timescale argument (Cox 1980; Winget & Kepler 2008). As the star cools, the base of the outer convection zone moves inwards, whereby the thermal timescale becomes increasingly higher there. Since the modes that can be excited have periods similar to the thermal timescale at the basis of the convection zone, modes with progressively longer periods (i.e., with higher radial orders) are excited as the star cools. When we shut down the ε mechanism, the g_1-mode becomes stable for the complete range (or part) of effective temperatures analyzed. This indicates that these modes are excited to a great extent by the ε mechanism through the hydrogen-burning shell. Higher radial-order modes, on the other hand, are insensitive to the effects of nuclear burning, and remain unstable due only to the $\kappa - \gamma$ mechanism.

Figure 1 shows the evolutionary tracks of all our white dwarf sequences in the $\log T_{\mathrm{eff}} - \log g$ diagram. Red thick segments on the evolutionary tracks indicate white dwarf models with the dipole g_1-mode excited mostly by the ε mechanism. The figure shows that low-mass white dwarfs evolved from progenitor stars characterized by metallicities in the range $0.00003 \lesssim Z \lesssim 0.001$ are expected to undergo g-mode pulsations powered by nuclear burning at the typical effective temperatures of ZZ Ceti stars. Nevertheless, in white dwarf models derived from solar metallicity progenitors (right-hand lower panel), which are indeed representative of ZZ Ceti stars (which are located in the solar neighborhood), nuclear burning does not play a role, and the ε-mechanism is not operative. For the case of white dwarf models evolved from progenitors with $Z = 0.0001$ (left-hand upper panel), we have explored the efficiency of the ε-mechanism by changing stellar masses, and found that for models more massive than $\sim 0.71\,M_\odot$, no g-modes are excited by nuclear burning. In Fig. 1 we have indicated the empirical blue edge of the ZZ Ceti instability strip according to Gianninas et al. (2011). Clearly, models having the pulsationally unstable g_1-mode excited by the ε mechanism are located in (or near) the ZZ Ceti instability domain. The g_1-mode found to be unstable in our computations is not merely excited by the ε mechanism, but also by the $\kappa - \gamma$ mechanism, which contributes somewhat to its destabilization.

Furthermore, we include in Fig. 1 the location of the theoretical end of the instability domain of pre-white-dwarf models with hydrogen-rich envelope, as predicted by Maeda & Shibahashi (2014). Note that, at variance with the ε-destabilized g_1-mode found in this paper in the ZZ Ceti instability domain, the unstable modes in the pre-white-dwarf models considered by Maeda & Shibahashi (2014) are excited only by the ε mechanism. This is because at those high effective temperatures and luminosities, hydrogen is completely ionized at the surface layers, hence the $\kappa - \gamma$ mechanism is inhibited. We have performed additional stability computations to investigate whether g-modes are excited by the ε mechanism at higher luminosities. For these exploratory computations, we have considered a template white dwarf evolutionary sequence with $M_\star = 0.535\,M_\odot$ and progenitor metallicity $Z = 0.0001$, from $T_{\mathrm{eff}} \sim 100\,000$ K downwards. We found that dipole modes g_1, g_2, g_3 and g_4 are excited by the ε mechanism due to hydrogen burning down to an effective temperature of $\sim 36\,000$ K. These results are in line with those obtained by Maeda & Shibahashi (2014), although the instability domain obtained here extends to lower effective temperatures, by virtue that our white dwarf models are characterized by more vigorous hydrogen burning. A full exploration of the instability domain at high luminosities by varying the stellar mass and the metallicity of the progenitors is, however, beyond the scope of this paper, and will be presented in a future publication.
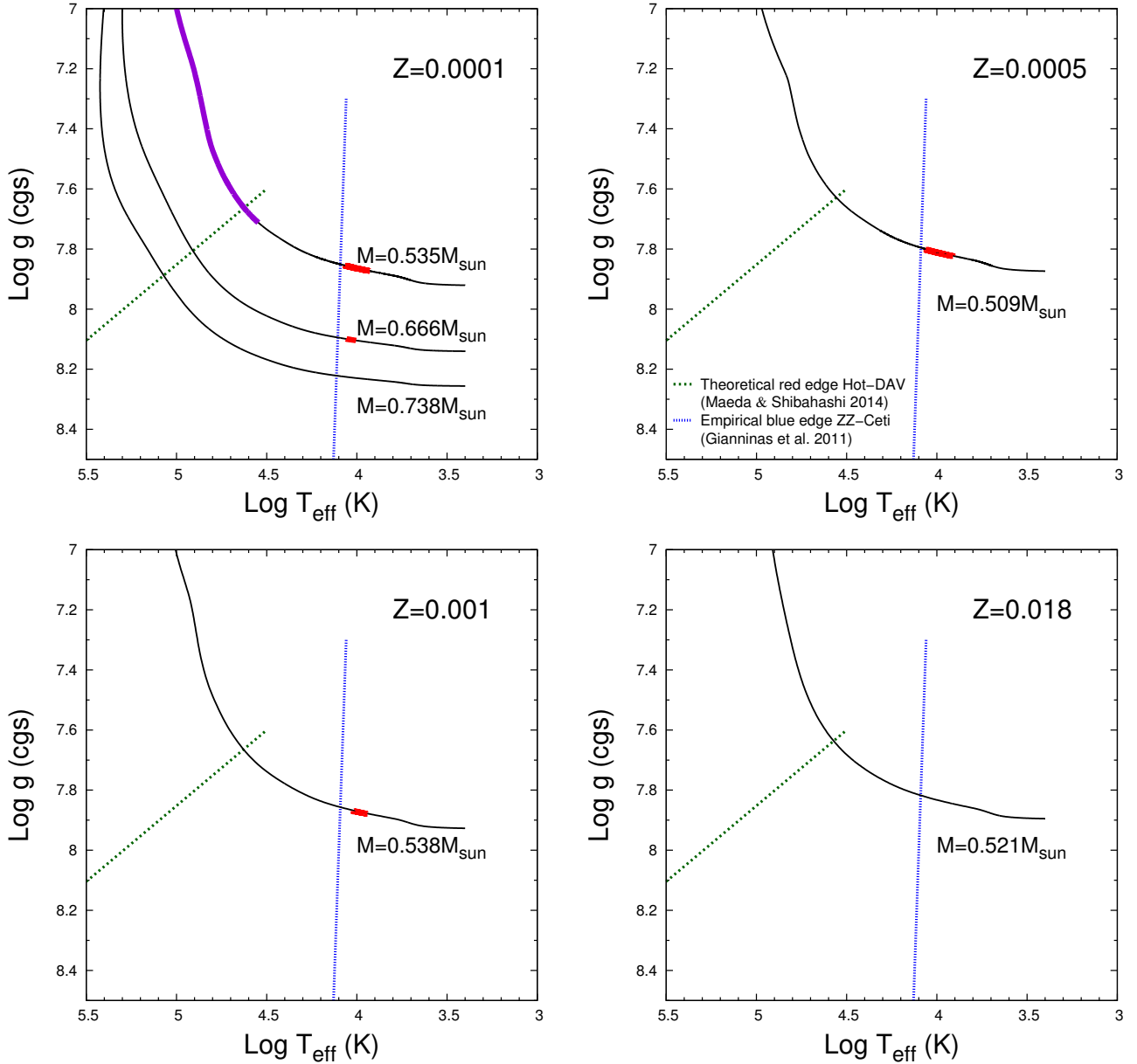
Fig. 1. Evolutionary tracks of white dwarf models with $M_\star \sim 0.51-0.54\,M_\odot$ on the $\log T_{\rm eff}-\log g$ plane. Each panel corresponds to a different metallicity value (Z) of the white dwarf progenitors. For the case of $Z = 0.0001$ we include two additional sequences with masses $M_\star = 0.666\,M_\odot$ and $M_\star = 0.738\,M_\odot$. Red thick segments on the tracks at $\log T_{\rm eff} \sim 4$ correspond to DA white dwarf models having the dipole g_1-mode destabilized mostly by the ε mechanism acting at the hydrogen burning shell. The violet thick segment in the case of the $M_\star = 0.535\,M_\odot$ and $Z = 0.0001$ sequence corresponds to models with unstable low-order g-modes (g_1 to g_4) destabilized solely by the ε mechanism. The dashed green line indicates the theoretical red edge of the instability domain of pre-white-dwarfs with hydrogen-rich envelopes evolved from $M_{\rm ZAMS} \geq 1.5\,M_\odot$ with solar metallicity found by Maeda & Shibahashi (2014). The almost vertical dotted blue line corresponds to the empirical blue edge of the instability domain of ZZ Ceti stars reported by Gianninas et al. (2011).

Figure 2 shows the unstable periods of dipole g-modes in terms of the effective temperature for our white dwarf model sequence with $M_\star = 0.535\,M_\odot$ and $Z = 0.0001$. The left panel shows the results for the standard nonadiabatic pulsation computations. A dense spectrum of g-modes is destabilized by the $\kappa - \gamma$ mechanism for effective temperatures below $\sim 11\,800-11\,400$ K. The right panel corresponds to the same sequence but for the case in which the ε mechanism is artificially inhibited, and consequently, only the $\kappa-\gamma$ mechanism is allowed to act. The e-folding time (in years) of each unstable mode, defined as $\tau_{\rm e} = 1/|\Im(\sigma)|$, where $\Im(\sigma)$ is the imaginary part of the complex eigenfrequency σ, is also indicated. The e-folding time is a measure of the time taken for the perturbation to reach an observable amplitude. For the $M_\star = 0.535\,M_\odot$ and $Z = 0.0001$ sequence, the dipole g_1-mode is unstable in the standard computations (left panel), but the mode becomes stable when we neglect the effect of nuclear energy production on stability (right panel). Hence, we conclude that the mode is unstable due to the ε mechanism. The e-folding time of this mode is shown in terms of the effective temperature in Fig 3. When the ε mechanism is allowed to operate, the e-folding time is about 5×10^6 yr, whereas the time the star needs to cross the instability domain is of about 1.2×10^9 yr. Therefore, if the nuclear energy production is as intense as our models predict, the dipole g_1-mode has enough time to reach observable amplitudes while the star is still evolving in that effective temperature range. A similar situation
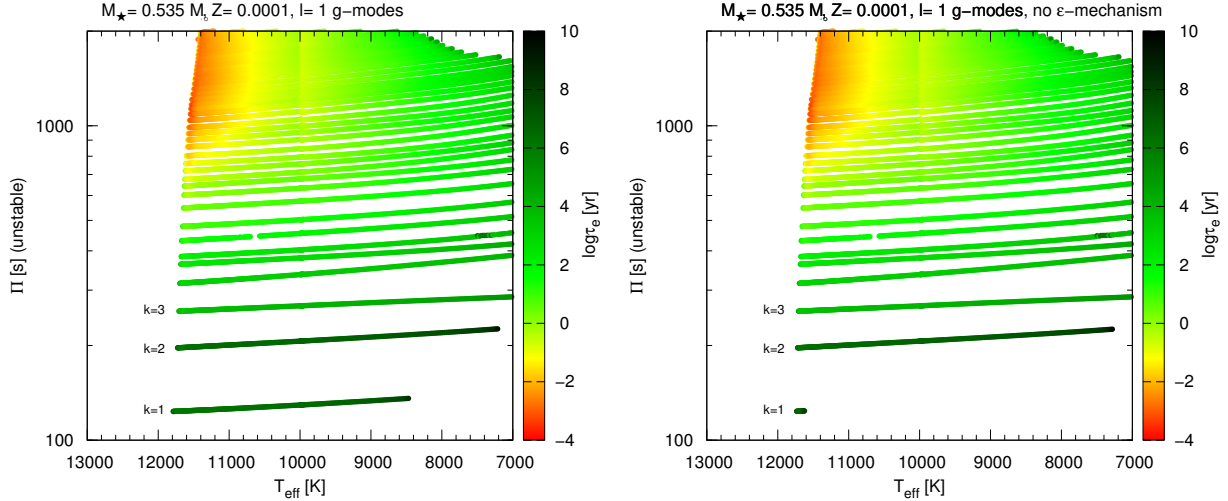
Fig. 2. Periods (Π) of unstable dipole g-modes in terms of the effective temperature for our white dwarf model sequence with $M_\star = 0.535 M_\odot$ and $Z = 0.0001$. The *left panel* corresponds to the sequence in which the ε mechanism was allowed to operate, whereas in the *right panel* we show the situation in which it was artificially suppressed. Color coding indicates the e-folding time (τ_e) of each unstable mode (right scale).
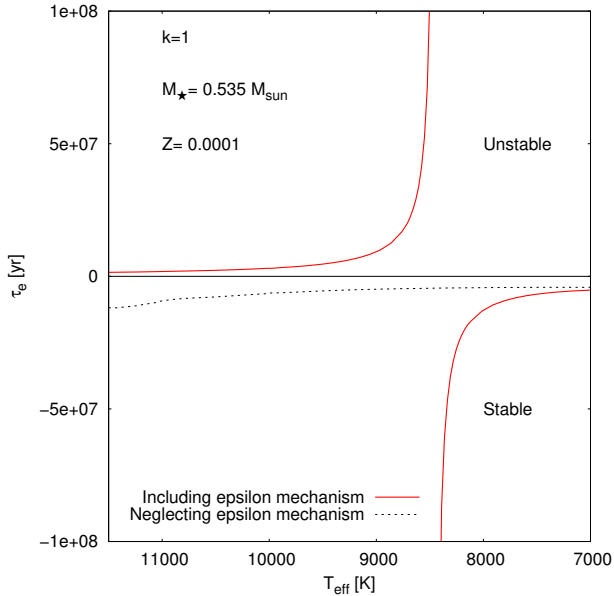
Fig. 3. e-folding time of the g_1-mode of our $M_\star = 0.535 M_\odot$ and $Z = 0.0001$ white dwarf sequence, in terms of the effective temperature.

is found for the white dwarf models evolved from progenitors with $Z = 0.0005$ and $Z = 0.001$ sequences, as shown in the upper right and the lower left panels of Fig. 1, respectively. In these cases, however, the efficiency of the ε mechanism is lower (due to less vigorous nuclear burning), and as a result, the ranges in T_{eff} in which the dipole g_1-mode is destabilized by this mechanism are narrower. In the extreme case of white dwarfs evolved from solar-metallicity progenitors, that mode is found to be no longer excited by the ε mechanism. This result is expected because, for these white dwarfs, nuclear burning plays a minor role at advanced stages of their evolution.

We also performed nonadiabatic computations for white dwarf models with $M_\star = 0.666 M_\odot$ and $M_\star = 0.738 M_\odot$ coming from progenitors with $Z = 0.0001$. For the $0.666 M_\odot$ sequence, we still found that the dipole g_1-mode is unstable mostly due to the ε mechanism, although for a narrow range of effective temperatures (see the upper left panel of Fig. 1). However,

for the $0.738 M_\odot$ sequence, we found that mode no longer excited by the ε mechanism. Again, this is an expected result, since no appreciable nuclear burning occurs in these models (see Althaus et al. 2015), and because the progenitor star of this sequence experienced carbon enrichment in the AGB phase due to third dredge-up episodes, as revealed in the C/O ratio listed in Table 1. We have estimated the expected threshold mass (M_T) above which the epsilon mechanism is not operative anymore. Specifically, we artificially reduce the nuclear energy release in the $0.666 M_\odot$ sequence down to a value below which the epsilon mechanism is not able to excite the g_1 pulsation mode, and then we use the corresponding nuclear luminosity at which this occurs to interpolate between our $0.666 M_\odot$ and $0.738 M_\odot$ sequences to find M_T. The stellar mass value turns out to be $M_T \approx 0.71 M_\odot$.

We now examine which regions of the models contribute to the driving and damping of a given pulsation mode. Figure 4 shows the Lagrangian perturbation of the temperature ($\delta T/T$) for the dipole g_1-mode (upper left-hand panel) and the g_3-mode (lower left-hand panel), respectively, corresponding to a $Z = 0.0001$, $M_\star = 0.535 M_\odot$ template model at $T_{\mathrm{eff}} = 11\,000$ K. For the g_1-mode, the eigenfunction $\delta T/T$ has a local maximum at $\log(1 - M_r/M_\star) \sim -3.5$, where the hydrogen-burning shell is located. The ε mechanism acts as a filter that provides substantial driving to those g-modes that have a maximum of $\delta T/T$ in the region of the nuclear burning shell. For the dipole g_3-mode, on the other hand, $\delta T/T$ has negligible values at the burning shell region, hence the ε mechanism does not provide efficient driving for this mode.

It is useful to introduce the running work integral $W(r)$, which represents the work done on the overlying layer by the sphere of radius r (see Unno et al. 1989). Its surface value, $W := W(R)$, gives the increase of the total energy over one period of oscillation. If $W > 0$, the pulsation is gaining energy in one cycle, which means that the mode is unstable and grows. Otherwise, if $W < 0$, the mode is losing energy and damps. The derivative of $W(r)$ gives us information about the regions of driving and damping of the oscillations. Regions in the star where $dW(r)/dr > 0$ will contribute to driving, and zones in which $dW(r)/dr < 0$ will provide damping.

We show $dW(r)/dr$ for the dipole g_1-mode in the middle upper panel of Fig. 4 for the cases when the ε mechanism is allowed and inhibited to operate. The ε mechanism provides significant
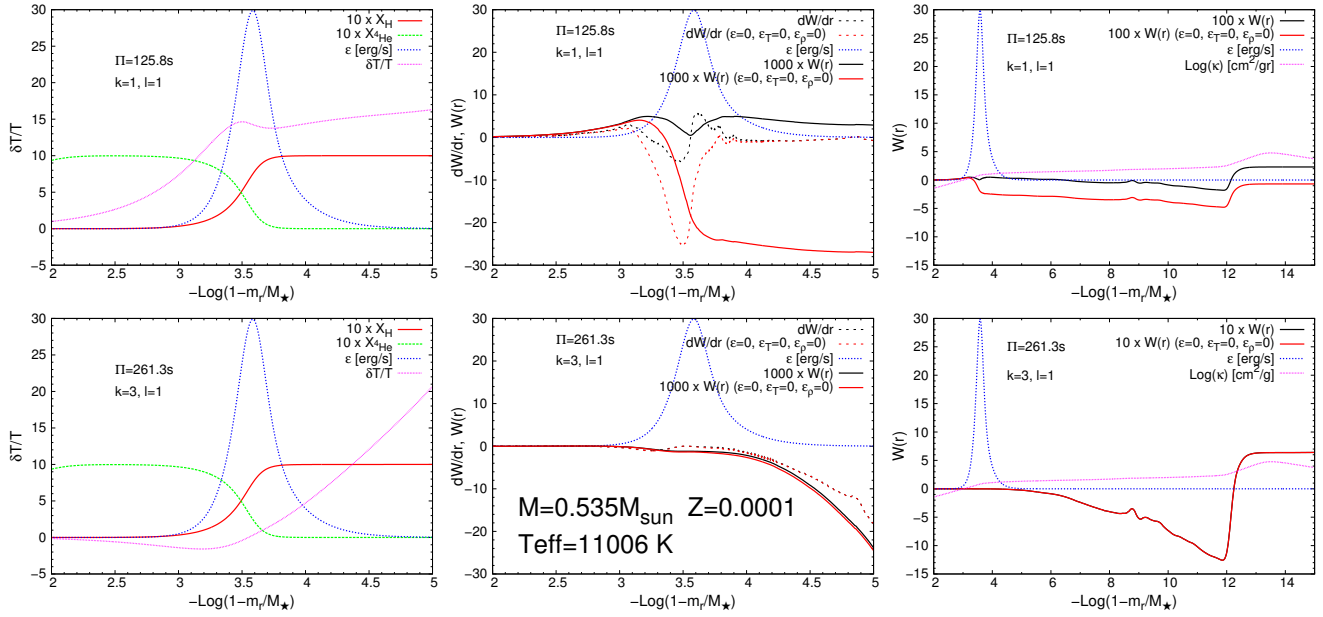
Fig. 4. *Left panels*: Lagrangian perturbation of temperature ($\delta T/T$), nuclear generation rate (ε), and the mass fractions of hydrogen and helium (X_H and X_{He}, respectively) as functions of $\log(1 - M_r/M_\star)$ for dipole g_1-mode (*upper panel*) and g_3-mode (*lower panel*), respectively, for the model with $Z = 0.0001$, $M_\star = 0.535\,M_\odot$ and $T_{eff} = 11\,000$ K. The eigenfunction is normalized so that the relative displacement in the radial direction is unity at the stellar surface. *Middle panels*: same as *left panels* but for the differential work function ($dW(r)/dr$) for the case in which the ε mechanism is allowed to operate (black dashed curves) and when it is suppressed (red dashed curves). Also, the scaled running work integrals ($W(r)$) are shown with solid lines. *Right panels*: same as central panels, but the scaled running work integrals are shown for a wider range of the mass coordinate, along with the Rosseland mean opacity κ (radiative plus conductive).

driving at the hydrogen burning shell region, but substantial damping occurs there when the mechanism is inhibited. As a result, the running work integral $W(r)$ increases at the burning shell region when the ε mechanism operates, while it substantially decreases when the mechanism is switched of. As can be seen in the right-hand upper panel of this figure, when ε mechanism operates, $W(r)$ becomes positive at the surface of the star, thanks to the driving contribution due to the $\kappa - \gamma$ mechanism, and the g_1-mode becomes globally unstable. In contrast, when the ε mechanism is inhibited, the driving contribution by the $\kappa - \gamma$ mechanism cannot prevent that $W(r)$ becomes negative at the surface, making the g_1-mode stable in these circumstances.

On the other hand, for the dipole g_3-mode (lower panels of Fig. 4), no significant driving is provided at the hydrogen burning shell region. However, since substantial driving occurs in the hydrogen-ionization zone due to the $\kappa - \gamma$ mechanism, $W(r)$ becomes positive at the surface. Thus, the g_3-mode is unstable, regardless of whether nuclear burning is taken into account or not in the stability computations.

4. Summary and conclusions

Althaus et al. (2015) predicted that low-mass white dwarfs – evolved from low metallicity progenitors that did not experience carbon enrichment due to third dredge-up episodes during the AGB phase – are born with hydrogen envelopes thick enough to develop intense hydrogen shell burning at low luminosities ($\log(L/L_\odot) \lesssim -3$). Following these results, in this paper, we have investigated whether g-modes in DA white dwarfs could be unstable due to the ε mechanism powered by the hydrogen burning shell. For that purpose, we computed nonadiabatic pulsation modes of white dwarf models with $M_\star \sim 0.51-0.54\,M_\odot$, evolved from progenitorial stars with four different metallicities: $Z = 0.0001$, $Z = 0.0005$, $Z = 0.001$, and $Z = 0.018$.

The first three sequences correspond to low-metallicity stellar populations, while the latter one is representative of objects in the solar neighborhood. We have found that for the white dwarf sequences evolved from low-metallicity progenitors, both dipole and quadrupole g_1-modes are unstable mostly due to the ε mechanism acting at the hydrogen burning shell. We found that the ability of this mechanism to destabilize those pulsation modes decreases with increasing metallicity. In the limit of white dwarfs with solar metallicity progenitors ($Z = 0.018$), no pulsation is driven by the ε mechanism, since nuclear burning does not play a role in these objects. We also explored the mass dependence of the ε mechanism efficiency, by computing white dwarf sequences with higher masses ($M_\star = 0.666\,M_\odot$ and $M_\star = 0.738\,M_\odot$) evolved from $Z = 0.0001$ progenitors. Our calculations showed that the ε mechanism destabilizes both the dipole and quadrupole g_1-modes associated with the $0.666\,M_\odot$ sequence, but does not excite these modes for the sequence with $M_\star = 0.738\,M_\odot$.

To summarize, hydrogen shell burning in DA white dwarfs at effective temperatures typical of the instability strip of ZZ Ceti stars triggers the dipole ($\ell = 1$) and the quadrupole ($\ell = 2$) g_1-modes with period $\Pi \sim 70-120$ s, provided that the mass of the white dwarf is $M_\star \lesssim 0.71\,M_\odot$ and the metallicity of the progenitor stars is in the range $0.0001 \lesssim Z \lesssim 0.001$. The e-folding times for these modes are much shorter than the evolutionary timescale, which means that they could have enough time to reach observable amplitudes. We hope that, in the future, these modes can be detected in white dwarfs in low-metallicity environments, such as globular clusters and/or the galactic halo, allowing us to place constraints on nuclear burning in the envelopes of low-mass white dwarfs with low-metallicity. Moreover, detection of these pulsation modes could eventually verify that low-metallicity AGB stars do not experience carbon enrichment due to third dredge-up episodes. Once again,

asteroseismology of white dwarfs can prove to be a powerful tool to sound the interior of these ancient stars, and also to constrain the history of their progenitors.

References

Althaus, L. G., Serenelli, A. M., Córsico, A. H., & Montgomery, M. H. 2003, A&A, 404, 593

Althaus, L. G., Serenelli, A. M., Panei, J. A., et al. 2005, A&A, 435, 631

Althaus, L. G., Córsico, A. H., Isern, J., & García-Berro, E. 2010, A&ARv, 18, 471

Althaus, L. G., García-Berro, E., Isern, J., Córsico, A. H., & Miller Bertolami, M. M. 2012, A&A, 537, A33

Althaus, L. G., Camisassa, M. E., Miller Bertolami, M. M., Córsico, A. H., & García-Berro, E. 2015, A&A, 576, A9

Brickhill, A. J. 1983, MNRAS, 204, 537

Camisassa, M. E., Althaus, L. G., Córsico, A. H., et al. 2016, ApJ, 823, 158

Cassisi, S., Potekhin, A. Y., Pietrinferni, A., Catelan, M., & Salaris, M. 2007, ApJ, 661, 1094

Castanheira, B. G., & Kepler, S. O. 2008, MNRAS, 385, 430

Castanheira, B. G., & Kepler, S. O. 2009, MNRAS, 396, 1709

Cojocaru, R., Torres, S., Althaus, L. G., Isern, J., & García-Berro, E. 2015, A&A, 581, A108

Córsico, A. H., & Althaus, L. G. 2014, ApJ, 793, L17

Córsico, A. H., & Althaus, L. G. 2016, A&A, 585, A1

Córsico, A. H., Althaus, L. G., & Miller Bertolami, M. M. 2006, A&A, 458, 259

Córsico, A. H., Althaus, L. G., Miller Bertolami, M. M., González Pérez, J. M., & Kepler, S. O. 2009, ApJ, 701, 1008

Cox, J. P. 1980, Theory of stellar pulsation (Princeton N. J. Princeton University Press)

Ferguson, J. W., Alexander, D. R., Allard, F., et al. 2005, ApJ, 623, 585

Fontaine, G., & Brassard, P. 2008, PASP, 120, 1043

Fontaine, G., Brassard, P., Charpinet, S., Randall, S. K., & Van Grootel, V. 2013, in Progress in Physics of the Sun and Stars: A New Era in Helio- and Asteroseismology, eds. H. Shibahashi, & A. E. Lynas-Gray, ASP Conf. Ser., 479, 211

Gianninas, A., Bergeron, P., & Ruiz, M. T. 2011, ApJ, 743, 138

Goldreich, P., & Wu, Y. 1999, ApJ, 511, 904

Groenewegen, M. A. T., Whitelock, P. A., Smith, C. H., & Kerschbaum, F. 1998, MNRAS, 293, 18

Groenewegen, M. A. T., Sloan, G. C., Soszyński, I., & Petersen, E. A. 2009, A&A, 506, 1277

Iglesias, C. A., & Rogers, F. J. 1996, ApJ, 464, 943

Kawaler, S. D., Winget, D. E., Hansen, C. J., & Iben, Jr., I. 1986, ApJ, 306, L41

Maeda, K., & Shibahashi, H. 2014, PASJ, 66, 76

Magni, G., & Mazzitelli, I. 1979, A&A, 72, 134

Miller Bertolami, M. M., Althaus, L. G., & García-Berro, E. 2013, ApJ, 775, L22

Rohrmann, R. D., Althaus, L. G., García-Berro, E., Córsico, A. H., & Miller Bertolami, M. M. 2012, A&A, 546, A119

Romero, A. D., Córsico, A. H., Althaus, L. G., et al. 2012, MNRAS, 420, 1462

Romero, A. D., Kepler, S. O., Córsico, A. H., Althaus, L. G., & Fraga, L. 2013, ApJ, 779, 58

Romero, A. D., Campos, F., & Kepler, S. O. 2015, MNRAS, 450, 3708

Saio, H. 2013, in Eur. Phys. J. Web Conf., 43, 05005

Schröder, K.-P., & Cuntz, M. 2005, ApJ, 630, L73

Segretain, L., Chabrier, G., Hernanz, M., et al. 1994, ApJ, 434, 641

Torres, S., García-Berro, E., Althaus, L. G., & Camisassa, M. E. 2015, A&A, 581, A90

Unno, W., Osaki, Y., Ando, H., Saio, H., & Shibahashi, H. 1989, Nonradial oscillations of stars, 2nd edn. (Tokyo: University of Tokyo Press)

Van Grootel, V., Dupret, M.-A., Fontaine, G., et al. 2012, A&A, 539, A87

Weiss, A., & Ferguson, J. W. 2009, A&A, 508, 1343

Winget, D. E., & Kepler, S. O. 2008, ARA&A, 46, 157